FLUORESCENT DERIVATIVES OF NUCLEOTIDES

METAL ION INTERACTIONS AND pH DEPENDENCY

J. M. VANDERKOOI, C. J. WEISS, AND G. V. WOODROW III,
Department of Biochemistry and Biophysics, University of Pennsylvania, Philadelphia, Pennsylvania 19104 U.S.A.

ABSTRACT The fluorescence parameters of ethenoadenosine derivatives are influenced by metal cations and pH, as summarized here. The pH profile of ethenoadenosine determined by fluorescence intensity gives a normal titration curve and is not affected by ionic strength. In contrast, the pH titration curves of etheno-ATP, etheno ADP, and etheno AMP depend upon ionic strength. At high ionic strength normal curves are obtained, whereas at low ionic strength anomalies are obtained; this suggests that the phosphates can interact with the ring, possibly by hydrogen bonding to the ring nitrogens. The room temperature fluorescence of ethenoadenosine occurs from the base form, although excitation of either the acid or base forms can contribute to the emission. This result can be explained if the excited state pK is lower than the ground state pK, and if deprotonation occurs within the time scale of the excited state. At low pH values the fluorescence lifetime of the base form is dependent upon the buffer concentration, indicating that the reverse reaction, protonation, occurs. The affinity constants for the binding of metals to the ethenoadenosine phosphates resemble those for the corresponding adenosine phosphates. Ni(II) and Co(II) are more effective than Mn(II) in quenching the fluorescence of ethenoadenosine phosphates; this result is predicted by Förster's theory for energy transfer based upon the overlap between donor emission spectrum and acceptor absorption spectrum. The diamagnetic ions Mg(II), Ca(II), and Zn(II) do not appear to affect the fluorescence of the ethenoadenosine phosphates directly, but rather to affect the conformation of the molecule, thereby affecting the quantum yield.

INTRODUCTION

The ethenoadenosine phosphates, introduced by Secrist and co-workers (1972), have been shown to substitute for the respective adenosine phosphate in a variety of enzymes. Because of their high fluorescence quantum yield and long fluorescent lifetime, the ethenoadenosine phosphates are useful probes of the nucleotide binding site.

The ethenoadenosine phosphates, like their adenosine parents, undergo a variety of reactions. In this report we describe the influence of pH and metal complexion on the fluorescence parameter of ethenoadenosine. The rationale for these experiments is that an understanding of the kinds of reactions the ethenoadenosine phosphates undergo in solution should allow interpretation of the fluorescence response when bound to an enzyme.

Dr. Weiss's permanent address is Northwestern College, Orange City, Iowa 51041.

A preliminary report was given at the Biophysical Discussions, (1978. *Biophys. J.* **24**:266–267).

METHODS

Ethenoadenosine derivatives were purchased from Sigma Chemical Co. (St. Louis, Mo.). They each showed one spot on thin-layer chromatography having the same mobility as the respective adenosine phosphate when using isopropanol:NH_4OH:$H_2O_{(6:1:3)}$ as solvent.

Other reagents were of analytical quality. Distilled water was used throughout.

Steady state fluorescence measurements were made using a Perkin-Elmer MPF-2A spectrofluorometer equipped with an R106 photomultiplier (Perkin-Elmer Corp., Instrument Div., Norwalk, Conn.).

Fluorescence decay measurements were made on a single photocounting instrument similar to the one described by Ygeurabide (1975). The cell compartment, gated lamp, and photomultiplier were obtained from Photochemical Research Associate (London, Ontario, Canada). Excitation and emission wavelengths were isolated using filters with absorption characteristics shown in Fig. 1. The data from the multichannel analyzer (LeCroy Research Systems Corp., St. Joseph, Mich.) was transferred to a Hewlett-Packard 9825A computer (Hewlett-Packard Co., Palo Alto, Calif.), where it was analyzed for the exponential decay rate according to Gafni et al. (1975) by Laplace transform.

Absorption spectra were obtained with a Perkin-Elmer Hitachi 200 spectrophotometer.

Energy transfer was calculated on basis of spectral overlap on basis of Förster's theory. The distance, R_0, at which 50% of the energy of the donor is transferred to the acceptor is:

$$R_0 = 9.79 \times 10^3 (Jn^{-4}\phi K^2)^{1/6}, \quad (1)$$

where J is the overlap between the donor emission spectrum and the acceptor absorption spectrum (Förster, 1949). The quantum yield of the donor, ϕ, was taken to be 0.56 (Secrist et al., 1972), and n, the refractive index, was taken to be 1.4. As pointed out previously (Vanderkooi et al., 1977), the possible range in values of the orientation factor, K^2, depends upon the symmetry of the donor and acceptor molecules. The components of the absorption band for a free metal ion are triply degenerate. The absorption spectrum of ATP complexed with Ni, Mn, or Co does not show splitting, therefore the transitions for the bound form should also be approximately triply degenerate. Therefore

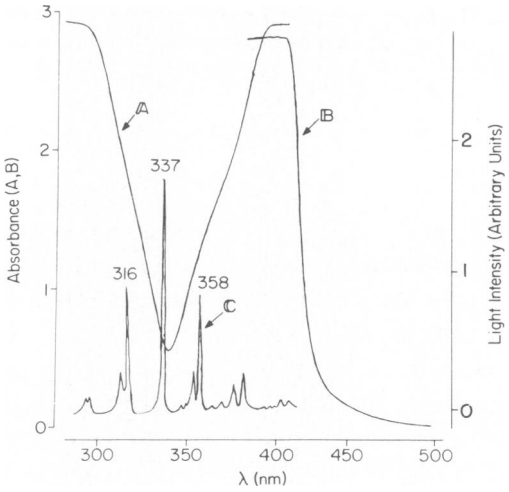

FIGURE 1 Wavelength selection for fluorescence decay measurement. *A*. Absorbance of Balzers R-UV 341-14 interference filter (Balzers High Vacuum Corp., Santa Ana, Calif.) used in the excitation beam. *B*. Absorbance of Corning CS3144 (Corning Glass Works, Science Products Div., Corning, N.Y.) plus Wratten 2E filters used in the emission beam. *C*. Light intensity of lamp (adapted from the manual, Photochemical Associates).

it is reasonable to use an orientation factor K^2 of $\frac{2}{3}$ for the calculation. This is the same orientation factor taken by Horrocks et al. (1975) and Latt et al. (1975) for energy transfer to complexed transition metal, based upon similar reasoning.

The calculated values for R_0 for ethenoadenosine and transition metal ion are 10.2 Å for Ni (uncomplexed), 9.6 Å for Co (uncomplexed), 11.4 Å for Ni (complexed to ATP), and 10.7 Å for Co (complexed to ATP).

The ethenoadenosine phosphate concentration was varied in the range of 0.2–10 μM in most experiments. The same results were obtained at all concentrations, indicating that there is no aggregation of the fluorescent probe.

Temperature for all experiments was ambient (~22°C) unless otherwise indicated.

Titrations with metals were done in distilled water (pH 6.5–7) to eliminate any reactions of the metal with the buffer. The pH was checked during the titrations to ascertain that it did not change. Titrations done in 10 mM Tris or Tris (hydroxymethyl) aminomethane (THAM)[1] buffers gave essentially the same results. The nucleotide-metal binding data were analyzed according to a generalized Adair equation (Adair, 1925):

$$A = A_0 + \frac{\sum_{i=1}^{N} \left(E_i [L]^i \prod_{j=1}^{i} K_j \right)}{1 + \sum_{i=1}^{N} \left([L]^i \prod_{j=1}^{i} K_j \right)}$$

$$E_i = \sum_{j=1}^{i} \xi_j [P_0], \tag{2}$$

where A is the observed fluorescence, A_0 is the fluorescence at zero ligand concentration, L is the concentration of free ligand, K_j is macroscopic binding constants, ξ is the increment in extinction at the j^{th} site (or class of identical sites), P_0 is the total concentration of substrate, and N is the number of binding sites (or classes of identical binding sites).

This generalized equation allows for unequal contributions to the fluorescence by each binding site (or class of identical binding sites). We may define this contribution as

$$C_j = \frac{E_i - E_{i-1}}{\sum_{j=1}^{N} | E_j - E_{j-1} |} \quad (E_0 = 0). \tag{3}$$

If the contributions of each site are identical, the binding equation reduces to the familiar Adair equation (Adair, 1925).

Analysis of the data by means of this equation was carried out by the nonlinear squares method of Rubin (Rubin, 1963). This is a modified Newton-Raphson method. Calculations were carried out on a Hewlett-Packard calculator, model 9825A, using a 9862A plotter and matrix, general input/output, extended input/output, and plotter read-only memory. The calculations reported here used less than 8K of random-access memory. The times required for analysis varied according to the number of parameters to be fit and the suitability of the initial guesses; they ranged from 15 s to about 3 min.[2]

---

[1] *Abbreviations used in this paper:* ethenoadenosine, 1,N^6-ethenoadenosine; etheno ADP, 1,N^6-ethenoadenosine-5'-diphosphate; etheno AMP, 1,N^6-ethenoadenosine-5'-monophosphate; etheno ATP, 1,N^6-ethenoadenosine-5'-triphosphate; HEPES, N-2-hydroxyethylpiperazine-*N'*-2- ethanesulfonic acid; THAM, Tris (hydroxymethyl) aminomethane.

[2] A copy of the program, with documentation, is available from the author.

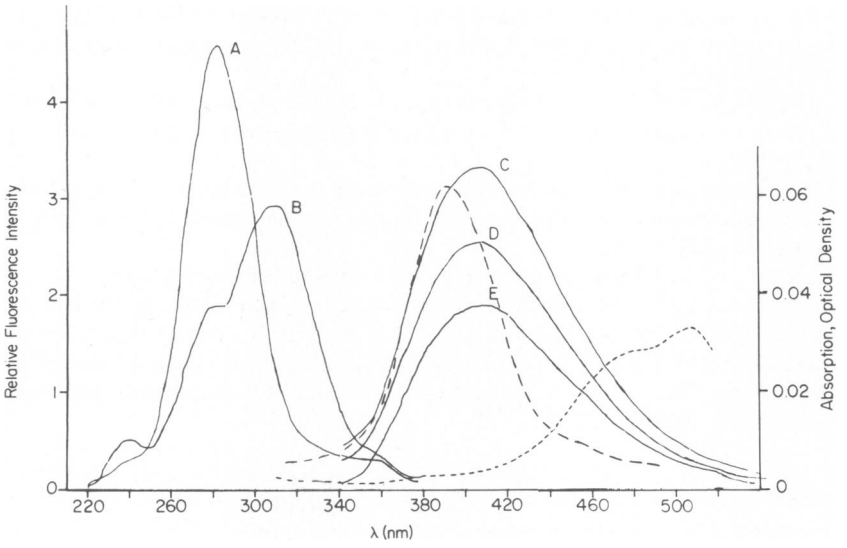

FIGURE 2 Excitation and emission spectra of ethenoadenosine (--) 1 M etheno ATP in 0.1 M THAM at: *A*. pH 2.5, emission wavelength, 404 nm; *B*. pH 5.6 emission wavelength, 404 nm; *C*. pH 2.5 excitation wavelength, 308 nm; *D*. pH 5.6 excitation wavelength, 308 nm and *E*. pH 5.6, excitation wavelength, 280 nm. (— — —) Absorption spectrum of 0.02 M $NiCl_2$; (- - - - -) Absorption spectrum of 0.01 M $CoCl_2$.

RESULTS

The spectra presented in Fig. 2 illustrate two features of ethenoadenosine fluorescence that serve as starting points for our experiments. First of all, the excitation spectrum is different at pH 2.5 and 5.6, while the emission spectrum of ethenoadenosine is independent of pH. This is an indication that the excited state and ground state pK's differ. Secondly, the absorption spectrum of the transition metals Ni(II) and Co(II) overlap with the emission spectrum of ethenoadenosine. This suggests the possibility that Förster energy transfer, which depends upon spectral overlap, can be used to monitor interactions between the nucleotide phosphate and the metal.

The pH Dependency of Ethenoadenosine Phosphates

Secrist et al. (1972) have characterized the absorption and fluorescence spectra of ethenoadenosine derivatives with regard to viscosity and polarity of solvent, pH, and temperature. They observed that the absorption spectrum shows a clear isobestic point at 294 nm with variation in pH. The pK_a for the ethenoadenosine derivatives was reported by them to be around 3.9. We have duplicated their results, but would like to point out several additional effects of pH on these derivatives.

The titration curves for ethenoadenosine and etheno ATP in 5 mM $MgCl_2$ are presented in Fig. 3. The fluorescence intensity was measured by using 318 nm as excitation wavelength, ensuring that only the basic form is excited. The pK for ethenoadenosine is 3.86, and for Mg ethenoATP is 4.4. Examination of the data in Fig. 3 shows that the ethenoadenosine titration curve deviates slightly from a simple sigmoidal titration curve, and that the data could be better fit using two pK's: 2.52 (17% contribution) and 3.96 (83% contribution).

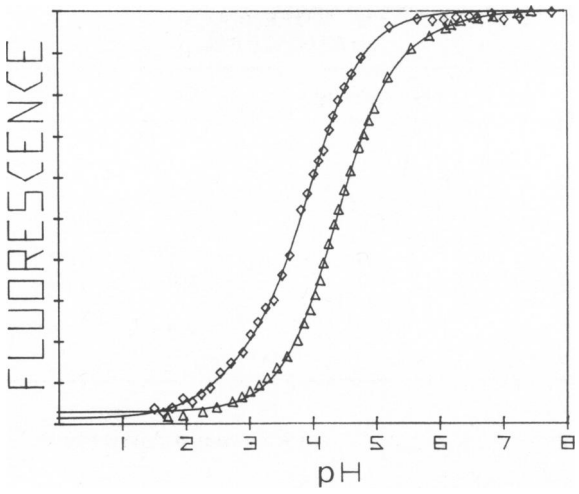

FIGURE 3 pH titration of ethenoadenosine and etheno ATP: ◇ 1 μM ethenoadenosine; △ 1 μM etheno ATP, 5 mM $MgCl_2$. Excitation: 318 nm; emission 420 nm. Symbols are experimental points; lines are theoretical curves based on computer best fit. Constants are given in Table I.

This small component could be due to an excited state protonation reaction, as is described later. The pH profile of etheno ATP was the same when $CaCl_2$ (5 mM) or KCl (0.1 or 1.0 M) was substituted for $MgCl_2$.

In contrast to the simple binding curves observed under conditions given in the legend of Fig. 3, the titration curves of the ethenoadenosine phosphates at low ionic strength show marked deviation from simple proton binding. The data for etheno ATP and etheno AMP could be fit using two binding constants (Fig. 4). The pK values for etheno ATP are 4.45 and

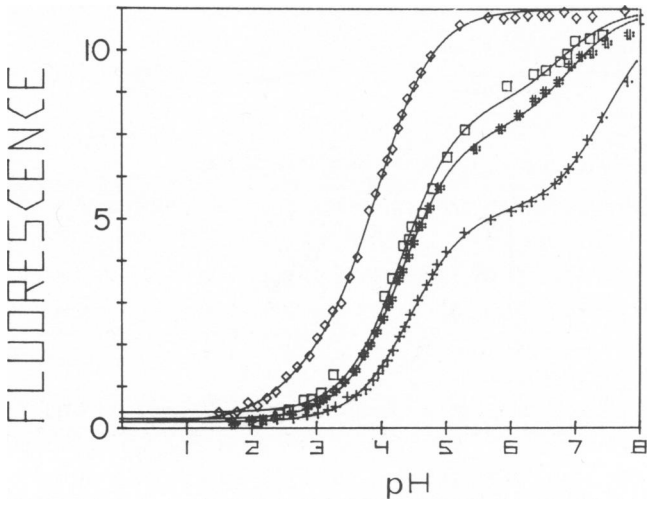

FIGURE 4 pH titration at low ionic strength: + 1 M etheno ATP; □ 1 M etheno ADP; # 1 M etheno AMP; ◇ 1 M ethenoadenosine. Excitation: 318 nm; emission 420 nm. Lines are theoretical curves of computer best fit. Constants are given in Table I.

TABLE I
pH TITRATIONS

	Ethenoadenosine	AMP	ADP	ATP
Species 1				
pK	2.52	—	—	—
Contribution, %	16.9			
Species 2				
pK	3.96	4.29	4.31	4.45
Contribution, %	83.1	60.6	76.6	51.7
Species 3				
pK	—	6.9	6.79	7.48
Contribution, %		29.4	23.4	48.3

7.48, for etheno ADP are 4.31 and 6.79, and for etheno AMP are 4.29 and 6.9. These results are summarized in Table I.

The diminished fluorescence yield of the ethenoadenosine phosphates at intermediate pH values could be explained by complex formation between the phosphate and either the ground state or the excited state. In the former case the absorption spectrum, and possibly also the excitation spectrum, would be affected, while in the latter case the emission decay

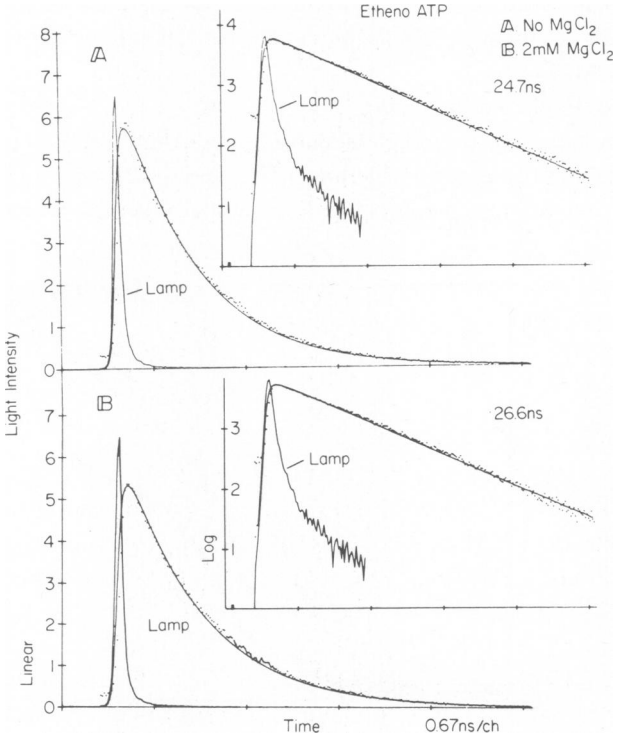

FIGURE 5 Fluorescence decay of etheno ATP. *A*. Fluorescence decay of etheno ATP, 2 μM; points are data, line is computer fit of 24.7 ns. Mean of three determinations was 24.6 ± 0.2. *B*. Fluorescence decay of etheno ATP, 2 μM in 2 mM $MgCl_2$. Line is computer fit of 26.6 ns. Time scale: 0.67 ns/channel, 170 ns full scale. Mean of three determinations was 26.7 ± 0.3. Insert: Semi-log display.

rate would be changed. We could detect no change in the absorption spectrum or excitation spectrum of etheno ATP when Mg Cl_2 (5 mM) was added. However, a small change in fluorescent lifetime was observed when Mg was complexed to etheno ATP (Fig. 5), indicating that the quenching is due at least in part to an excited state complex.

Additional information concerning the pH dependency of ethenoadenosine can be obtained by considering the kinds of reactions that an excited state molecule can undergo.

The Excited State pK of Ethenoadenosine

Weber (1931) first observed that fluorescent molecules with dissociable hydrogens could show an anomalous dependence on pH of the fluorescence spectra. It is now well established that this phenomenon can be attributed to a difference in pK_a of the ground and excited states (Förster, 1950; Weller, 1952, 1961; DeLucas et al. 1971). The following scheme applies:

$$\begin{array}{ccccc} & & \overset{pK^*}{\underset{k_{-1}}{\overset{k_1^*}{\rightleftharpoons}}} & & \\ H_2O & + \; AH^* & & A^* & + \; H_3O^+ \\ \uparrow\downarrow & & & \uparrow\downarrow & \uparrow\downarrow \\ & k_{fH} + k_{NRH} & & & k_f + k_{NR} \\ \uparrow\downarrow & & & \uparrow\downarrow & \uparrow\downarrow \\ H_2O & + \; AH & \overset{pK}{\rightleftharpoons} & A & + \; H_3O^+, \end{array} \tag{4}$$

where the asterisk (*) denotes excited state, AH is the protonated form, A is the basic form, k_f and k_{fH} are the rate of fluorescence decay for A* and AH*, k_{NR} and k_{NRH} are the nonradiative decay rates for A* and AH*, respectively.

Parker (1968) points out that the difference in pK and pK* can be obtained either from the electronic excitation or emission spectra, by assuming that reaction entropies in the ground and in the excited state are the same.

The room temperature spectra for ethenoadenosine, given in Fig. 2, show that the difference in energy between the maximum wavelengths for excitation of the acid and base forms is 0.303 μm^{-1}; Parker calculates the pK* at 20°C to be

$$pK^* = pK - 21.4\,(\Delta\bar{\nu}). \tag{5}$$

This allows calculation of pK* to be −2.59.

Fluorescence from the acid form was not observed at room temperature at pH values above one. However, at low temperatures a luminescence with emission maximum at 345 nm was observed at acid pH (Fig. 6). (The weaker-structured luminescence between 380 and 500 nm is likely to be phosphorescence, arising from the excited triplet state.) Using the difference in energy between the maximum wavelengths, the excited state pK is also calculated to be below the ground state pK.

While it is clear that the excited state equilibrium favors the base form, equilibrium may not be obtained within the excited state lifetime. The following reactions can describe the kinetic properties of A*:

$$A^* + H_3O^+ \rightarrow A^*H + H_2O, \tag{6}$$

$$A^* + HB \rightarrow A^*H + B^-, \tag{7}$$

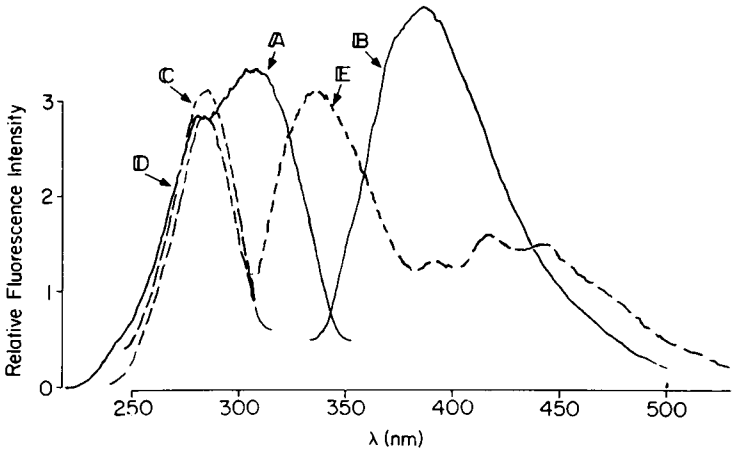

FIGURE 6 Low temperature luminescence spectra of ethenoadenosine. The sample contained 1 μM ethenoadenosine and 1 mM phosphate buffer at pH 7.0 (*A*, *B*) or pH 2 (*C*, *D*, *E*). *A*. Excitation spectrum, 400 nm emission wavelength; *B*. Emission spectrum, 308 nm excitation wavelength; *E*. Emission spectrum, 280 nm excitation wavelength; *C*, *D*, excitation spectrum, 340 nm (*C*) or 450 nm (*D*) emission wavelength. Temperature: 77°K.

$$A^* \rightarrow A + h\nu, \tag{8}$$

$$A^* \rightarrow A, \tag{9}$$

where B is a buffer. This sequence of reactions predicts that at high buffer concentration and high H_3O^+ concentration, the decay rate of A* will be a function of both.

It is demonstrated in Fig. 7 that the fluorescence decay rate of A* increases with increasing

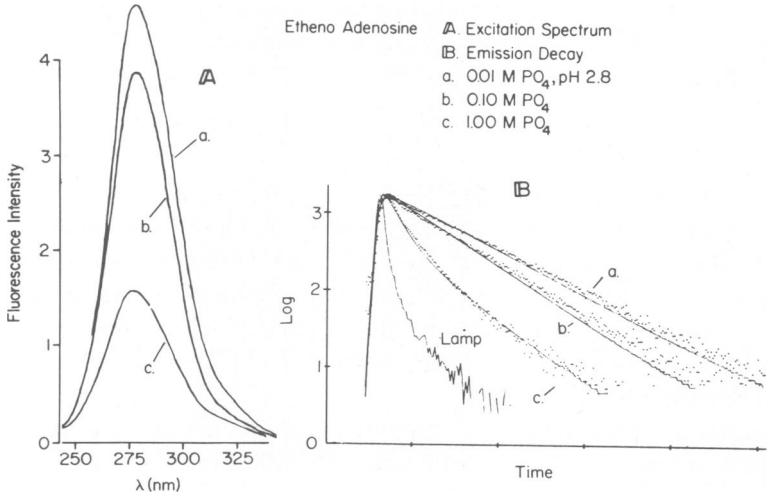

FIGURE 7 Fluorescence excitation spectrum and fluorescence decay profile of ethenoadenosine. The fluorescence excitation spectrum (*A*) or decay (*B*) of 1 μM adenosine in 0.01 M PO_4 buffer (*a*), 0.1 M phosphate buffer (*b*), or 1.0 M buffer (*c*) was obtained at 22°C. Solid line in *B* is computer fit of data giving 24.1 (*a*), 17.3 (*b*), and 7.9 (*c*) ns as fluorescent lifetimes.

phosphate buffer concentration. These results show that protonation of the excited state molecule can occur when H_3O^+ or HB concentrations are high (Eqs. 4 and 5).

In summary, the pH profiles of ethenoadenosine phosphates are anomalous. We propose that protonation of the excited state molecule by the phosphate may account for this. This observation is important since the quantum yield of ethenoadenosine, when bound to an enzyme, may be affected by dissociable hydrogens at the active site.

Metal Ion Interactions with Ethenoadenosine Derivatives

The fluorescence yields of ethenoadenosine derivatives are diminished in the presence of the transition metal ions Ni(II), Co(II), and Mn(II). The steady state fluorescence intensity profiles are given in Fig. 8. Two types of quenching can be distinguished: collisional quenching

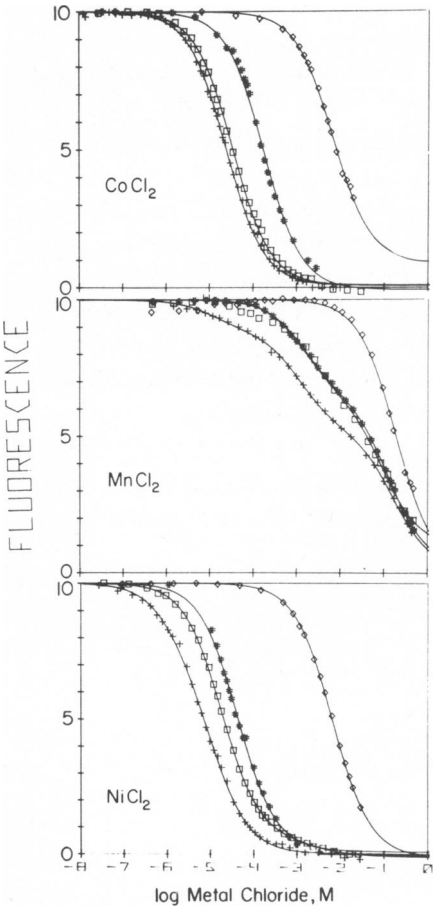

FIGURE 8

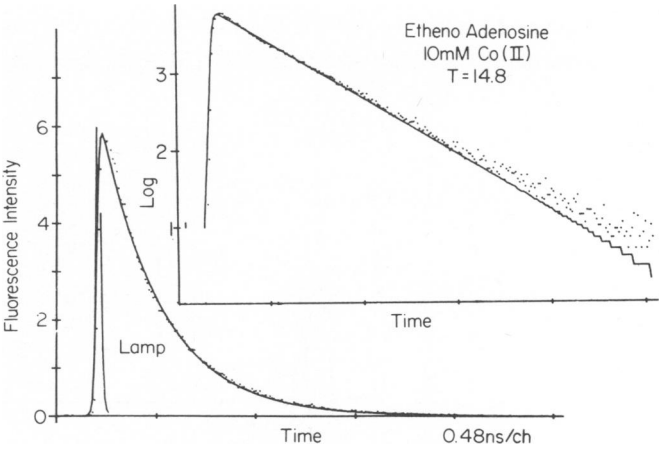

FIGURE 9

FIGURE 8 Effect of transition metal ions on the fluorescence intensity of ethenoadenosine phosphate. The sample contained 1 μM etheno ATP (+), etheno ADP (□), etheno AMP (#) or ethenoadenosine (◇), and metal acetate in concentration given on the figure. Excitation 318 nm; emission 420 nm; pH: 6.8. Temperature: 20–22°C.

FIGURE 9 Effect of cobalt acetate on fluorescence decay of ethenoadenosine. 1 μM ethenoadenosine in 10 mM Co acetate. Solid line: computer fit, τ = 14.8 ns.

and complex formation. "Collisional" quenching occurs when the diffusion coefficient and the quencher concentration are sufficiently large so that encounters between the quencher and fluorochrome occur within the time scale of the excited state. Collisional quenching is described by the Stern-Volmer (1919) relationship:

$$\frac{\tau_o}{\tau} = \frac{F_o}{F} = 1 + k\tau_o[Q], \tag{10}$$

where k is the diffusion-limited rate constant, Fo and τ_o are the respective fluorescence yields and lifetimes in the absence of quencher, Q, and F and τ are the respective yields and lifetimes in the presence of quencher. It is apparent that with increasing quencher concentration, the fluorescent lifetime, τ, will decrease in proportion to the fluorescent yield. This was observed for Co (Fig. 9) and Ni (not shown), providing strong evidence that quenching of ethenoadenosine by these ions occurred by a collisional process.

High concentrations of Mn also quench the fluorescence of ethenoadenosine. In contrast to the fluorescence decay of ethenoadenosine in the presence of Ni or Co, the decay is biphasic in the presence of Mn (Fig. 10). This could be due to steric hinderence of "soft-core" collisions.

Low concentrations of Ni(II), Mn(II), or Co(II) are effective in quenching ethenoadenosine phosphate fluorescence. This is an indication of complex formation. In addition, the fluorescent lifetime of etheno ATP at concentrations of Co or Ni where 50% quenching occurs is the same as in the absence of metal cations; this indicates that only the uncomplexed form fluoresces. The calculated distance, R_0, for Förster energy transfer is 11.4 A for Ni(II), and 10.7 A for Co(II) to ethenoadenosine. These distances are of the order of the size of the complex and therefore the complexed form of the ethenoadenosine phosphate is expected to be totally quenched.

Unlike Ni and Co, Mn(II) has little spectral overlap with ethenoadenosine (Fig. 2); it is consequently not unexpected that the Mn-adenosine phosphate is still fluorescent, but with

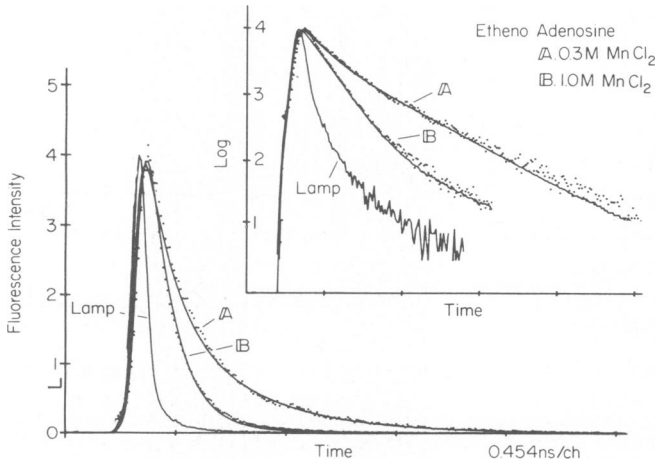

FIGURE 10 Fluorescence decay of ethenoadenosine in the presence of $MnCl_2$. 1 M ethenoadenosine in *A*. 0.3 M $MnCl_2$ or *B*. 1.0 M $MnCl_2$. Temperature: 20°C, pH; 6.8. Solid lines are computer-simulated decay curves using 7.1 and 18 ns as decay times for *A*, and 3.0 and 15 ns for *B*.

TABLE II

STABILITY CONSTANTS OF ADENINE NUCLEOTIDES AND ETHENOADENOSINE NUCLEOTIDES

Metal		Etheno-adenosine	Etheno AMP	AMP	Etheno ADP	ADP	Etheno ATP	ATP
Ni	Species 1, pK	2.19			2.56			
	contribution, %	100			6.3			
	Species 2, pK		4.36	2.84	4.73	4.50	4.901	
	contribution, %		100		93.7		69.7	
	Species 3, pK						5.8	5.32
	contribution, %						30.3	
	Reference	*	*	‡	*	‡	*	§
Co	pK	2.18	3.76	2.64	4.46	4.20	4.61	5.21
	Reference	*	*	‡	*	‡	*	§
Mn	Species 1, pK	0.72	0.87		1.02		0.775	
	contribution, %	100	64.2		61.8		48	
	Species 2, pK		2.84	2.40	2.87	4.16	2.93	
	contribution, %		35.8		38.2		36.4	
	Species 3, pK						4.90	4.78
	contribution, %						11.9	
	Reference	*	*	‡	*	‡	*	‡

*This work

‡Taqui, Khan, M. M., and A. E. Martell. (1967). *J. Am. Chem. Soc.* **89**:5585 (pH titration method)

§Perrin, D. D., and V. S. Sharma. (1966). *Biochim. Biophys. Acta.* **127**:35 (pH titration method)

a decreased quantum yield. The fluorescent lifetime of Mn-etheno ATP is less than that of etheno ATP, also an indication that the complexed form is still fluorescent. However, the decay profile is complex, and could not be fit by two exponential decay parameters. Since the extent of quenching was a function of temperature, a kinetic factor may be involved in the quenching. This point is under investigation.

The affinities for the binding of metals to ethenoadenosine derivatives are summarized in Table II.

DISCUSSION

The binding affinities of metal cations for ethenoadenosine phosphate are similar to the affinities reported for the respective adenosine phosphates, as measured using a variety of physical techniques (Table II).

The diamagnetic ions Mg(II) and Ca(II) do not appear to affect the fluorescence of etheno-adenosine phosphates directly. The quenching by transition metal cations of excited singlet states has been attributed to Förster energy transfer in other systems (Latt et al., 1970; Horrocks et al., 1975). The quenching by manganese is probably due to a "paramagnetic" effect. The geometrical constraints for this reaction are not known, although the data presented in this paper show that Mn must be in close contact to be effective. Using the data given in Fig. 8 and Table II, we can estimate the distance. According to Stern and Volmer (1919), quenching can be considered as a pseudo-first order process, and k, the quenching rate constant, can be obtained. The Smoluchowski equation (1917) relates k, the rate constant, with encounter distance (r) and the diffusion coefficient of reactants

(D_A and D_B):

$$k = 4\pi Nr(D_A + D_B) \times 10^3, \quad (11)$$

where N is Avogadro's number. When assuming the radius, r, for Ni and Co to be the same as the radius of interaction, R_0, predicted by Förster's theory, the value for $(D_A + D_B)$ is 8.5×10^{-6} cm^2/s. This is a reasonable value for diffusion coefficient for small molecules and ions in aqueous medium (Krogh, 1920). If the diffusion coefficient is the same for all the transition ions, then the "radius of interaction" for Mn is under 0.5 Å. This is less than the sum of the ionic and molecular sizes of the two diffusants.

Several reasons may account for the multiple fluorescence decay times observed when Mn quenches ethenoadenosine fluorescence. First of all, Mn may form a weak ground state complex with ethenoadenosine. We did not, however, observe a difference in the absorption spectrum of ethenoadenosine in the presence of Mn. Another possibility may be due to the collisional quenching process itself. In the case of Förster transfer, the energy transfer is inversely dependent upon the sixth power of distance. Thus the quenching is effectively "hard-core," since when a molecule enters within the distance R_0 it is quenched. If the quenching is "soft-core," that is, if the quenching depends upon a lower power of distance, then the distribution of quenchers with differing quenching probabilities could lead to non-exponential decay. That the "radius of interaction" is less than the sum of the radius of the two diffusants does indicate geometrical constraints on the reaction. Finally, the general diffusion theory predicts that the fluorescence decay would be nonexponential since time is required to establish a diffusion gradient (Smoluchowski, 1919; Vanderkooi and Callis, 1974). This could not totally account for the biphascity in the decay curve, however, since the time required to establish a diffusion gradient in solution of low viscosity is small.

The differences in the quenching of ethenoadenosine derivatives by transition metals can be a potent tool for studying metal interactions with nucleotides at the active site of enzymes. For example, the data presented here indicates that Mn will affect the fluorescence of ethenoadenosine only when it is near the nucleotide binding site. On the other hand Co and Ni can quench fluorescence over longer distances, and therefore when they bind at sites removed from the adenosine ring, they will still influence the fluorescence.

In addition to binding metals, the ethenoadenosine phosphates undergo excited state reactions interesting in themselves. The fluorescence yields of ethenoadenosine phosphates are decreased in the pH range where the gamma phosphate is protonated. Both the pH and ionic strength dependencies of the fluorescence are consistent with hydrogen bonding between a nitrogen and the phosphate; one possible configuration is shown in Fig. 11. If this

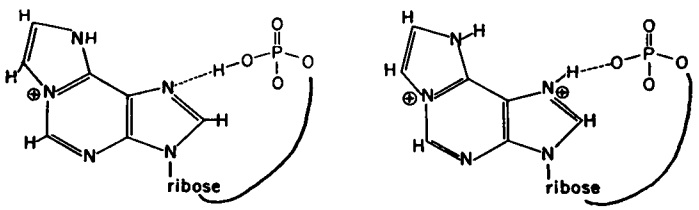

FIGURE 11 Possible hydrogen bond between phosphate and ring nitrogen.

mechanism is operative, it would imply that hydrogen exchange is very rapid, since the fluorescence decay profile could be fit with a single exponential (Fig. 5).

The reaction of the excited state ethenoadenosine with hydrogen donors has potential use in characterizing nucleotide binding sites. The observation that ethenoadenosine fluorescence is quenched when bound to some enzymes can indicate the existence of a hydrolyzable proton at the active site.

The authors wish to thank Dr. Ludwig Brand, Johns Hopkins University, for use of equipment in the early part of this work.

This research was supported by grants GM12202 and GM21699. J.M.V. was supported by a Research Career Development Award 5K04GM53.

Received for publication 20 April 1978 and in revised form 9 August 1978.

REFERENCES

ADAIR, G. S. 1925. The hemoglobin system. VI. The oxygen dissociation curve of hemoglobin. *J. Biol. Chem.* **63**:529.

DELUCA, M., L. BRAND, T. A. CEBULA, H. H. SELIGER, and A. F. MAKULA. 1971. Nanosecond time-resolved proton transfer studies with dehydroluciferin and its complex with luciferase. *J. Biol. Chem.* **246**:6702–6704.

FÖRSTER, T. 1950. Elektrolytische dissoziation angeragter molekule. *Z. Elektrochem.* **54**:42–46.

FÖRSTER, T. 1959. Transfer mechanisms of electron excitation. *Discuss. Faraday Soc.* **27**:7.

GAFNI, A., R. L. MODLIN, and L. BRAND. 1975. Analysis of fluorescence decay curves by means of the Laplace transformation. *Biophys. J.* **15**:263–280.

HORROCKS, W. D., B. HOLMQUIST, and B. L. VALLEE. 1975. Energy transfer between terbium (III) and cobalt (II) in thermolysin: a new class of metal-metal distance probes. *Proc. Natl. Acad. Sci. U.S.A.* **72**:4764–4768.

KROGH, A. 1929. Anatomic und physiologie der Capillarn. Q. Aufl. Springer-Verlag GmbH, Berlin, West Germany.

LATT, S. A., D. S. AULD, and B. L. VALLEE. 1970. Surveyor substrates: energy-transfer gauges of active center topography during catalysis. *Proc. Natl. Acad. Sci. U.S.A.* **67**:1383–1389.

PARKER, C. A. 1968. Photoluminescence of Solutions. Elsevier Scientific Publishing Company, Amsterdam. 361.

RUBIN, D. I. 1963. Nonlinear least squares parameter estimation and its application to chemical kinetics. *Chem. Eng. Prog. Symp. Ser.* **42**:59, 90–94.

SECRIST, J. A., J. R. BARRIO, N. J. LEONARD, and G. WEBER. 1972. Fluorescent modification of adenosine-containing coenzymes. Biological activities and spectroscopic properties. *Biochemistry.* **11**:3499–3505.

SMOLUCHOWSKI, M. 1917. Über Brownsche molekularbewegungunter Einwirkung ausser krafte und deren Zusammenhang mit der verallgemeinerten diffusiongleichung. *Z. Phys. Chem. (Leipz.) B.* **92**:129.

STERN, O., and M. VOLMER. 1919. Über die ablingungszeit der fluoreszenz. *Phys. Z.* **20**:183.

VANDERKOOI, J. M., and J. CALLIS. 1974. Pyrene a probe of lateral diffusion in the hydrophobic region of membranes. *Biochemistry.* **13**:4000.

VANDERKOOI, J. M., R. LANDESBERG, G. W. HAYDEN, and C. S. OWEN. 1977. Metal-free and metal-substituted cytochromes *c*. Use in characterization of the cytochrome *c* binding site. *Eur. J. Biochem.* **81**:339–347.

WEBER, K. 1931. Über die enge beslehung der fluorescenzausloschung zur hemmungphotochemischer reaktionen. *Z. Phys. Chem. (Leipz.) B.* **15**:18–44.

WELLER, A. 1952. Quantitative Untersuchungen der fluoreszenzumwaldlung bei naptholen. *Z. Elektrochem.* **56**: 662.

WELLER, A. 1961. Fast reactions of excited molecules. *Prog. React. Kinet.* **1**:187–214.

YGEURABIDE, J. 1972. Nanosecond fluorescence spectroscopy of macromolecules. *Methods Enzymol.* **26**:498–578.